Acta Geod Geophys (2016) 51:333–346
DOI 10.1007/s40328-015-0129-1

Coda Q in Eastern Indian shield

Prosanta K. Khan[1] · **Kuntal Bhukta**[1] · **Gaurab Tarafder**[1]

Received: 30 August 2014 / Accepted: 22 June 2015 / Published online: 5 July 2015

Abstract We have analyzed 16 earthquake waveform data recorded during the period from 2006 to 2013 at broadband station lying at the premises of Indian School of Mines, Dhanbad in the Eastern Indian Shield region. Coda window lengths of 30, 40 and 50 s were selected after thorough analysis of the waveforms. The Coda Q (Q_c) values were computed using single back scattered method. The earthquakes parameters were compiled from catalogue of Indian Meteorological Department (Nodal agency under Govt. of India for record keeping and data sharing), New Delhi. The estimated average Q_c values for three coda windows 30, 40 and 50 s are $Q_c = 259.1f^{0.808}$, $Q_c = 275.9f^{0.764}$ and $Q_c = 397.1f^{0.651}$, respectively. The average Q_c value estimated from the Q_c values for the time windows 30, 40 and 50 s is found to be $Q_c = 313.2f^{0.73}$. Thus, the attenuation follows the power law relationships (e.g., $Q_c = Q_0f^n$), and the moderate to higher values of frequency parameters (n) obviously show that the Q_c value is a strong function of frequency. The increasing values of Q_0 with increasing lapse time indicating the depth dependency of attenuation, and accounts for decreasing heterogeneity towards deeper level beneath the study area.

Keywords Attenuation of coda waves · Single back scattering method · Coda Q · Lapse time · Eastern India Shield

1 Introduction

During the propagation of seismic energy through the earth, its amplitude decays because of geometrical spreading, intrinsic and scattering attenuations. Intrinsic attenuation converts the seismic energy to heat due to inelastic absorption, and scattering attenuation redistributes the energy at random heterogeneities existing in the lithosphere. Therefore,

✉ Prosanta K. Khan
pkkhan_india@yahoo.com

1 Department of Applied Geophysics, Indian School of Mines, Dhanbad, India

the attenuation of seismic waves in the lithosphere is an important phenomenon for studying the diversity in the earth's physical property and seismic potential of the region (Singh and Herrmann 1983; Jin and Aki 1988; Parvez et al. 2008). Aki (1969) first paid attention to the continuous wave trains in the tail portion of the seismograms after the arrivals of all the direct waves, and termed them as "coda waves". Aki (1969, 1980) and Aki and Chouet (1975) proposed the coda of an earthquake is caused by the scattering of seismic waves and decay of the coda, characterized by the factor Q_c or coda Q, can be used to measure the attenuation in the lithosphere. The scattering is generally produced at irregular topography, complex surface geology, heterogeneous elastic property of the rocks, faults and cracks, which are more at the shallower level than the deeper parts of the lithosphere (Kumar et al. 2005). The frequency dependent relations for Q (Q_0f^n) have been developed for different regions of the world. The Q_0 values are found to be varied according to the tectonic activity and geological age of the regions. Aki (1980) found that the frequency dependency of Q increases with level of tectonic activity. Jin and Aki (1989) correlated the coda Q with the degree of fractures associated with the seismicity in the lithosphere. The spatial variation of coda Q in a region emphasizes for better understanding of tectonics, seismicity, seismic risk analysis and engineering seismology (Singh and Herrmann 1983; Jin and Aki 1988).

Q_c is computed using either a single or multiple scattering models (Aki and Chouet 1975; Sato 1977; Roecker et al. 1982; Van Eck 1988; Jin and Aki 1988; Hellweg et al. 1995; Mandal and Rastogi 1998). The single scattering model is based on backscattered body waves but not the primary waves, and estimates only the intrinsic attenuation factor (Q_i) (Pujades et al. 1991). While the multiple scattering model provides information regarding both primary and secondary wave attenuations, and gives the estimates of Q_i as well as scattering attenuation factor (Q_s) (Gao et al. 1983). Besides, the multiple scattering models include the effect of Q_i and Q_s separately to analyze the attenuation, instead of considering both the attenuation simultaneously. Wu and Aki (1988) reported that the simultaneous estimation of Q_i and Q_s may lead to large errors. Therefore, the single backscattering model is usually preferred for coda Q estimation. In the present study, we have used the single scattering model of Aki and Chouet (1975) to estimate the coda Q in the Eastern Indian Shield and adjoining regions. In this model the coda is supposed to be the superposition of backscattering wavelets from discrete scattering sources. Each wavelet is caused for a single scatterer in the absence of other scatterers. This scattering is considered as a weak scattering and Born approximation is done for neglecting the loss of energy from primary waves as well as the multiple scattering. Further, the coda is independent of source parameters, and coda wave principally depends on time for a fixed velocity in this model. It was observed that the coda spectrum of small earthquakes for near source is independent of earthquake size, epicentral distance and the path between station and hypocenter, and principally depends on lapse time (Aki and Chouet 1975; Sato 1977). We have carried out our analysis for three specific coda windows of 30, 40, and 50 s, where the noise levels were relatively less.

2 Tectonic setup

The Eastern Indian Shield, covering parts of south Bihar, north Orissa, south-western part of West Bengal and Jharkhand (Fig. 1), is constituted of several ovoid granitoid bodies of variable dimensions along with their enclaves and supracrustal envelopes (Bose 2009).

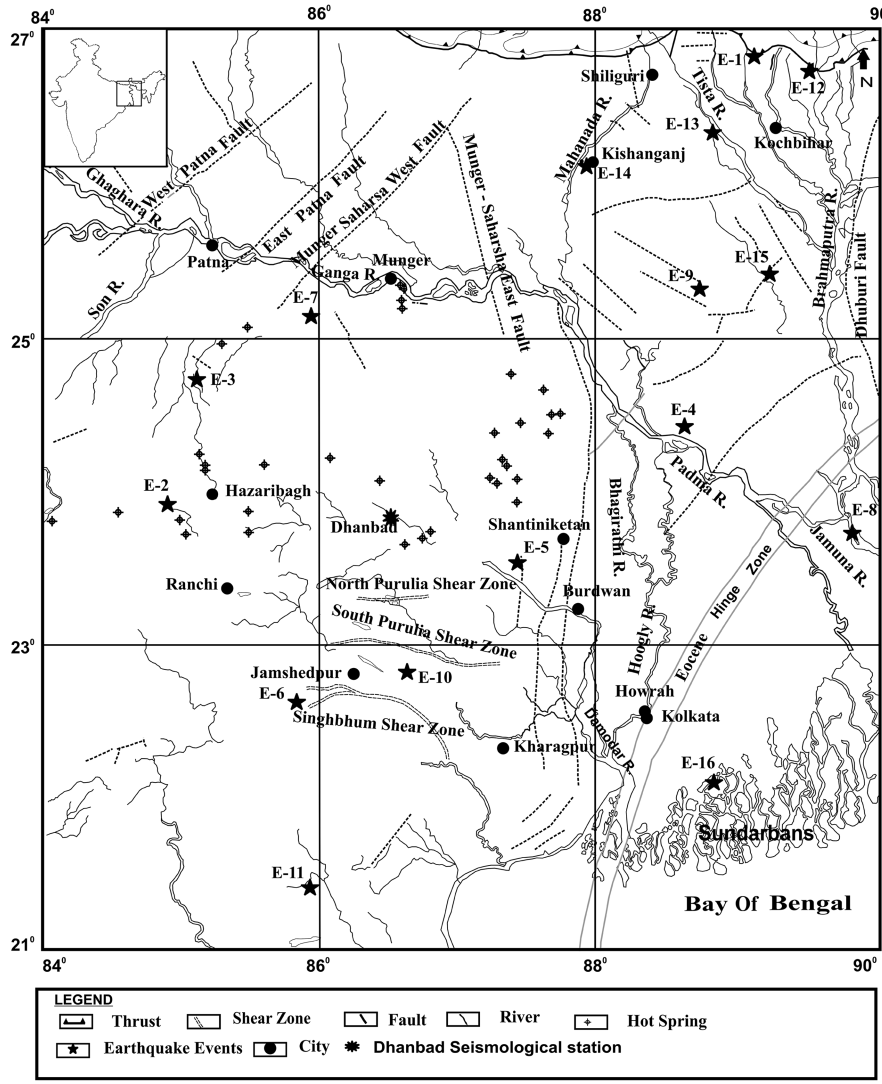

Fig. 1 Map shows the detailed tectonics and geological features of the Eastern Indian Shield Region. Epicenters of the analyzed earthquake events are shown by solid stars and numbers (E-1–E-16, Table 1)

This region was evolved through successive cycles of interactions of micro-plates with intervening periods of quiescence (Sarkar 1982). The quiescence periods were associated with both uplifts and intrusions of basic dyke swarms, and also erosion and paralic sedimentation, etc. (Bose 1999, 2009). The highest plateau is the Ranchi Plateau, comprising of dissected hills, located at $\sim$2000–3600 feet above the mean sea level, and separated by the Damodar trough from the Hazaribagh Plateau from north. The Chotanagpur Plateau, consisting mainly of gneisses and granite and partly of schists and other Dharwar rocks, represents an integral crustal segment of Precambrian high-grade metamorphic terrain of the central indian tectonic zone (CITZ) in the eastern part of the Indian Peninsular Shield

Table 1 Epicentral parameters and focal depths of 16 earthquake events used in the present attenuation study (cf. Fig. 1)

Sl. no.	Date	Origin time	Lat. (°N)	Long. (°E)	Focal depth (km)	Back Az. (°)	Epicentral dist. (km)	Mag. (M_L)
E-1	17-07-06	13:47:53	26.8	89.0	66	37	419	4.1
E-2	21-03-07	16:34:36	23.9	84.8	39	273	167	3.3
E-3	06-06-08	21:16:34	24.7	85.0	15	304	176	4.3
E-4	05-07-08	16:55:53	24.4	88.5	29.4	73	219	4.1
E-5	08-11-08	16:51:34	23.5	87.3	5	112	95	3.7
E-6	26-03-09	04:44:10	22.6	85.7	10	209	155	3.8
E-7	26-12-10	05:47:12	25.1	85.8	15	336	156	3.0
E-8	09-06-11	07:34:24	23.7	89.7	10	92	333	4.1
E-9	28-07-11	17:53:40	25.3	88.6	18	53	273	4.5
E-10	09-08-11	03:33:48	22.8	86.5	5	177	113	3.4
E-11	05-11-11	02:32:05	21.4	85.8	10	194	276	3.7
E-12	11-11-11	09:57:32	26.7	89.4	15	423	437	3.8
E-13	25-02-12	08:45:56	26.3	88.7	33	39	357	3.8
E-14	27-03-12	23:40:08	26.1	87.8	12	28	287	4.9
E-15	19-03-13	21:05:11	25.4	89.1	10	56	321	4.5
E-16	01-06-13	13:28:57	22.1	88.7	28	129	300	3.6

(Chatterjee and Ghose 2011; Bhattacharjee et al. 2012). The Ranchi, Hazaribagh and other smaller Plateaus are the integral part of the Chotanagpur Plateau. The other plateaus are the Rajmahal Hills and the Kaimur Plateau normally separated by narrow and steep slopes (e.g., scarps). It is believed that the Chotanagpur peneplain was uplifted thrice by the flexural response of the descending Indian lithosphere at the southern edge of the Himalayan deforming front since Tertiary times, and resulted the well-known waterfalls like Hundru, Jonha, etc. on its scarps. The first upliftment took place during the Eocene to Oligocene period creating the Pat region, the second one during Miocene forming the Ranchi and Hazaribagh Plateau and the third one during Pliocene and Pleistocene period uplifted the outer Chotanagpur Plateau. Another important oldest tectonic domain of this shield area is the Singhbhum craton comprising of granitoids and their enclaves (Naqvi and Rogers 1987; Weaver 1990), and surrounded by volcanosedimentary sequences, the supracrustals. Large-scale N-S displacements of the rocks along thrust belt have brought the Singhbhum craton and the Dalma volcanics in an intersecting disposition. It is appreciated in the literatures (Sarkar and Saha 1977; Sarkar et al. 1979) that the Singhbhum block, which lies to the southern part of the study region, is tectonically stable.

The present basement of the Eastern Indian Shield is unclassified gneissic complex, and sequences of Proterozoic fold belt crop out as isolated patches within the Chotanagpur Granite gneissic terrain. Sarkar and Saha (1977) reported that the compressional stress regime caused by northward convergence of the Singhbhum microplate against the continental margin of the Chotanagpur microplate led to the upliftment of the Chotanagpur granite-gneiss terrain, and initiated the reactivation of fractures during the Precambrian. These fractures in the gneissic basement recorded intrusions of mafic–ultramafic rocks, gabbro-anorthosite bodies, dyke swarms and granite plutons ranging in composition from ultramafic to acidic and sodic alkaline to ultrapotassic (Ghose and Mukherjee 2000; Ghose and Chatterjee 2008). Subsequently, an E-W trending intermontane trough was evolved, and later filled with fresh-water Gondwana sediments. Gondwana super group of rocks of the Damodar basin represents terrestrial facies cover in linear graben. Intermittent sedimentation over crystalline metamorphic rocks, synchronized subsidence and interspersed episodic deposition of coal measures greatly conditioned by climatic variations constitute the Gondwana basins (Sarkar 1982). Mahadevan (2002) revealed that a large number of hot springs locating in these areas apparently associated very closely with many of the fault zones. East of Rajmahal fault across the Ganga River is the Malda-Kishanganj fault that defines the western margin of the Rangpur saddle. Towards north of the study area the Gangetic foredeep, a downwarp of the Himalayan foreland, of variable depth, is converted into flat plains by long-vigorous sedimentation. This has shown considerable amounts of flexure and dislocation at the northern end near the foothills of the Himalaya (Bilham et al. 2003). The Himalayan Frontal Thrust, which runs across the southern border of Nepal, is identified by northward trending several faults and evenly spaced basement ridges (e.g., West and East Patna Faults, Munger-Saharsa Ridge Fault, Fig. 1) and few have shown evidence of movement during the Holocene epoch (Valdiya 1976; Dasgupta et al. 1987).

3 Data and methodology

We are running a digital broadband seismic station since December, 2006 at the premises of Indian School of Mines (ISM), Dhanbad. The station is located at latitude 23.82°N and longitude 86.44°E on the Archaean basement (hard rock terrain) of the Eastern Indian Shield. The elevation of the station is $\sim$247 m from the mean sea level. The station is recording continuously both local as well as regional earthquake events at 100 cycles/s over more than 7 years. We are also sharing our waveform data with the Indian Meteorological Department (IMD), a nodal agency under the Govt. of India, New Delhi. We here use 16 best recorded local events of local magnitude M_L 3.0 and above (Fig. 1; Table 1) for analyzing the coda wave attenuation in this part of Eastern India. The earthquake parameters of the 16 events have been taken from the IMD catalog. The waveform data recorded by the E-W and N-S components of the seismic sensor were analyzed separately for better understanding the coda wave characteristics. The Q values are computed through the CODAQ subroutine of SEISAN (seismic data processing software, Havskov and Ottemoller 2003). The time segment of the coda wave is usually selected at $t_{start} = 2t_s$ (t_s, the S-wave travel time) for ignoring the direct and forward scattering waves (Rautian and Khalturin 1978; Parvez et al. 2008). Mukhopadhyay and Sharma (2010) reported that $2t_s$ is the reliable coda starting time for local earthquakes as they did not find significant changes of Q_c values for 1.5, 2 and $2.5t_s$, respectively. We in the similar way have chosen a time window containing the coda of S wave starting at a lapse time equal to $2t_s$ (Fig. 2a) for calculation of $Q_c(f)$. The optimum coda window lengths of 30, 40 and 50 s are observed for all the events (Fig. 2b), and considered for Q_c analysis. The three coda windows are band-passed over 0.1–1.0, 1–5, 5–10, 10–15 and 15–25 Hz. The coda Q is estimated at respective central frequencies of the five frequency-bands adopting a single backscattering model (Aki and Chouet 1975), and finally, a relationship between A (f, t), f, Q_c and Q_0 is obtained (Fig. 2). The digital seismic data recorded by ISM broadband station are of high quality because the station is located on hard rock Archaean basement. We thus have not carried out noise analysis of the best recorded waveform digital data.

The coda waves have been modeled as a superposition of secondary waves through single back-scattering at randomly distributed heterogeneities (Aki 1969; Aki and Chouet

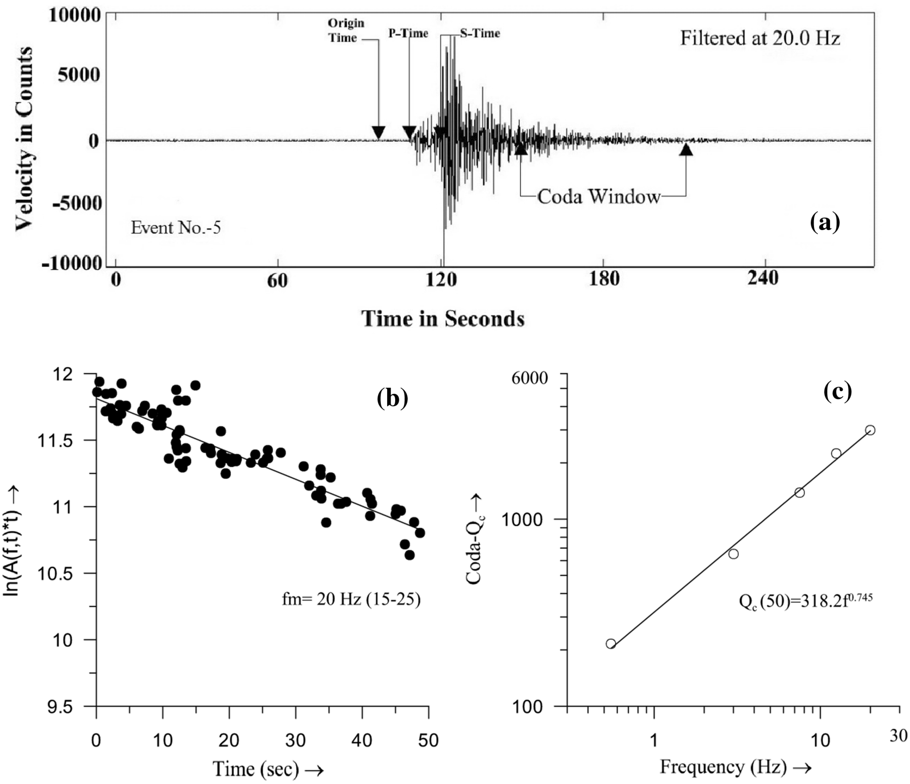

Fig. 2 **a** Band-pass filtered waveform data for earthquake event (No. E-5, Fig. 1; Table 1) recorded at ISM, Dhanbad station on 08-11-2008, **b** plotting of logarithmic of the product of RMS amplitude and corresponding lapse time (t) against t for event E-5, **c** plotting of quality factor against five central frequencies for the above event for coda windows of 30, 40 and 50 s, respectively

1975). The decrease of coda wave amplitude with lapse time at a particular frequency is only due to energy attenuation and geometrical spreading but independent of earthquake source, path propagation and site amplification (Aki 1969). Generally, the Q factor increases with frequency (Mitchell 1981) through the following relationship

$$Q = Q_0\left(\frac{f}{f_0}\right)^n$$

where Q_0 is the quality factor at the reference frequency f_0 (generally 1 Hz) and n is the frequency parameter, which is close to 1 and varies from region to region on the basis of heterogeneity of the medium (Aki 1981). In the present study, the attenuation of S-coda wave is calculated at five central frequencies after band-pass filtered using Butterworth five pole filters. The amplitude of the coda wave at lapse time t seconds from the origin time for band-pass filtered seismogram at central frequency f is given by the attenuation of the single back-scattering model as

$$A(f,t) \propto t^{-\alpha} e^{-\pi f t/Q_c}$$

or

$$A(f,t) = K(f)t^{-\alpha}e^{-\pi f t/Q_c} \quad (1)$$

where K (f) is the coda source factor at frequency f, which is independent of time and radiation pattern, α is the geometrical spreading parameter having one value out of 1.0, 0.5 or 0.75 for body waves, surface waves or diffusive waves, respectively (Sato and Fehler 1998), $Q_c(f)$ is the quality factor of coda waves. As coda waves are back-scattered body waves, therefore, putting $\alpha = 1$ in Eq. (1) and taking the logarithm,

$$\ln A(f,t) = \ln K(f) - \ln(t) - \frac{\pi f}{Q_c(f)}t$$

or

$$\ln(A(f,t)t) = \ln K(f) - \frac{\pi f}{Q_c(f)}t \quad (2)$$

Now, we obtain from Eq. (2)

$$Q_c(f) = \frac{\pi f}{b} \quad (3)$$

where b is the slope of the least squares straight line fit of plotting $\ln(A(f,\ t)t)$ against t (Fig. 2b) using the Eq. (2). The value of the term $A(f,\ t) \times t$ is obtained from the product of RMS amplitude and corresponding lapse time. Now, the Q_c is calculated using Eq. (3). The standard deviation of Q_c computed at each central frequency and frequency parameter is varied from one-fourth to one-third of the Q_c value for three intermediate frequency-band (i.e., 1–5, 5–10 and 10–15 Hz). While these are little higher for the lowest and highest frequency-bands (i.e., 0.1–1.0 and 15–25 Hz).

According to Rautian and Khalturin (1978), the above relation is valid for lapse time greater than twice the S-wave travel time for avoiding the data of the direct S-wave and for validation of the model that the source of the earthquake and receiver are coincident.

4 Results and discussion

The Q_c values have been estimated at five central frequencies 0.55, 3.0, 7.5, 12.5 and 20.0 Hz using the digital broadband waveform data. Optimum coda window length is selected from broadband data for sampling a considerable volume of the continental lithosphere. The window length of <20 s is generally undesirable except for short epicentral distances where the coda decay is rapid (Kvamme 1985). In the present study, the earthquake events are distributed sporadically at epicentral distances between 95 and 437 km (Table 1). We, therefore, choose three coda windows as 30, 40 and 50 s for proper sampling the volume of the lithosphere (Pulli 1984; Havskov et al. 1989) by back scattered wave beneath the study area.

The computed average Q_c values are plotted against central frequencies for the three different coda windows (Fig. 3). The Q_c values are usually found to be a function of frequency in the high-frequency range (1–24 Hz), and follow the power law relationships (e.g., $Q_c = Q_0 f^n$). The exponent n usually varies in the range 0.2–0.4 for higher values of Q_0 and close to unity for lower values (Udías 1999). Both Q_0 and n apparently represent the level of tectonic activity and degree of heterogeneities of the region (Kumar et al. 2007). The frequency dependency, based on the value of n, is directly correlated with the

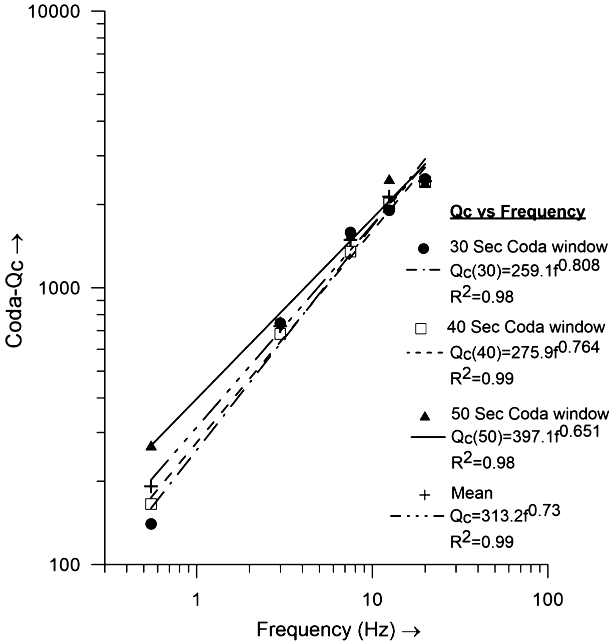

Fig. 3 Estimated average Coda Q showing frequency dependent relationship as $Q_c = Q_0 f^n$ for 30, 40 and 50 s coda windows

heterogeneities present in the subsurface (Roecker et al. 1982). The computed values of Q_0 and n lie between 259 and 397 and 0.808 and 0.651 for the three coda windows. The intermediate to higher values of n estimated here presumably indicate the overall moderate to higher level of tectonic activity for the study region. It was noted that the Q_c values increase with increasing frequencies for all the three time windows. According to Gao et al. (1983) the effects of multiple scattering are not important for local events with lapse time less than 100 s. The lapse time for the considered local events is less than 100 s, and the computed coda Q can apparently be attributed to the variation of attenuation with increasing depth.

A comparison of Q_c values calculated for the present study area with the existing Q_c values of other regions in India is shown in Fig. 4 and Table 2. Similar type of comparison for different regions of the world is explained in Fig. 5 and Table 3. It is found that the best-fitted line obtained here generally lies above that of Garhwal Himalaya (Gupta et al. 1995), North East India (Gupta and Kumar 2002), Andaman (Parvez et al. 2008), Koyna (Mandal and Rastogi 1998), and Kumaun Himalaya (Paul et al. 2003). On the other hand, the attenuation value is comparatively less than that of Indian Shield (Singh et al. 1999), Jabalpur Region (Singh et al. 2004), and Central India (Mandal et al. 2013) at low frequencies and gradually increases and exceeds at higher frequency. Although the attenuation value is greater than that of Sourashtra (Sharma et al. 2012), Kachchh (Sharma et al. 2008), and NW Himalaya (Kumar et al. 2005) at lower frequency, decreases marginally at higher frequency. In addition, the attenuation value though relatively greater than Himalayan arc (Singh et al. 2004) at lower frequency, both converges at higher frequency. It may be stated from the entire discussion that the study region accounts for moderate to higher attenuation of seismic shear wave.

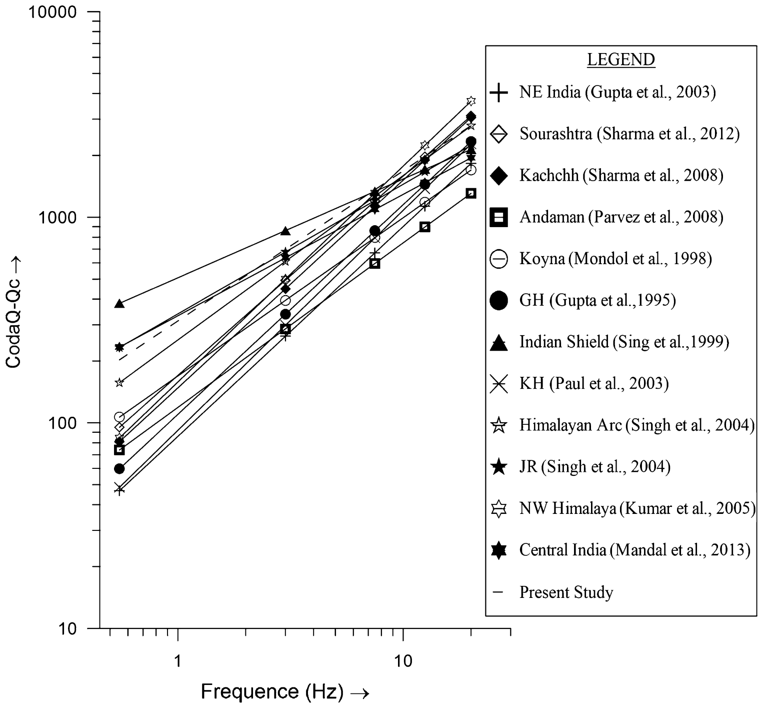

Fig. 4 Comparison of Q_c values between the Eastern Indian Shield and other regions of India. *NE* north east, *GH* Garhwal Himalaya, *KH* Kumaun Himalaya, *JR* Jabalpur Region

Table 2 Attenuation relationships ($Q_c = Q_0 f^n$) for different regions of India

Sl. no.	Region	$Q_{c=}Q_0\ f^n$	Author
1.	Northeast India	$86f^{1.02}$	Gupta and Kumar (2002)
2.	Sourashtra	$170f^{0.97}$	Sharma et al. (2012)
3.	Kachchh	$148f^{1.01}$	Sharma et al. (2008)
4.	Andaman	$119f^{0.8}$	Parvez et al. (2008)
5.	Koyna	$169f^{0.77}$	Mandal and Rastogi (1998)
6.	Garhwal Himalaya	$110f^{1.02}$	Gupta et al. (1995)
7.	Indian Shield	$508f^{0.48}$	Singh et al. (1999)
8.	Kumaun Himalaya	$92f^{1.07}$	Paul et al. (2003)
9.	Himalayan Arc	$253.f^{0.80}$	Singh et al. (2004)
10.	Jabalpur Region	$339f^{0.63}$	Singh et al. (2004)
11.	NW Himalaya	$158f^{1.05}$	Kumar et al. (2005)
12.	Central India	$332f^{0.59}$	Mandal et al. (2013)
13.	Eastern Indian Shield	$313.2f^{0.73}$	Present study

During worldwide comparison (Fig. 5), lesser attenuation relative to Eastern Canada (Chun et al. 1987; Shin and Herrmann 1987), Canadian Shield (Hasegawa 1985), Eastern United States (Gupta and McLaughlin 1987), Central Appalachia (Shi et al. 1996),

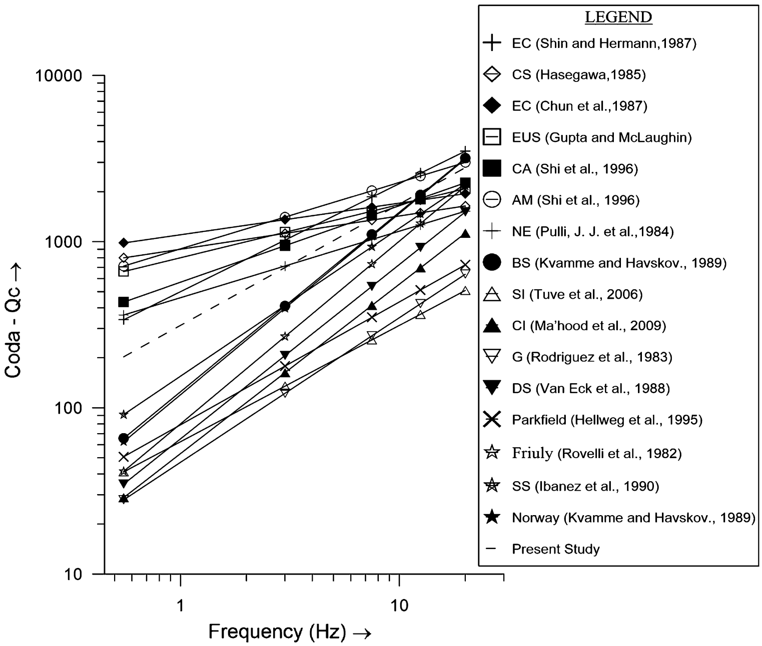

Fig. 5 Comparison of Q_c values between the Eastern Indian Shield and other regions around the world. *EC* Eastern Canada, *CS* Canadian shield, *EUS* Eastern United States, *CA* central Appalachia, *AM* Adirondack mountains, *NE* New England, BS baltic shield, *SI* Southern Italy, *CI* Central Iran, *G* Guerrero, *DS* Dead Sea, *SS* South Spain

Table 3 Attenuation relationships ($Q_c = Q_0 f^n$) for different regions around the world

Sl. no.	Region	$Q_c = Q_0 f^n$	Author
1.	Eastern Canada	$500f^{0.65}$	Shin and Herrmann (1987)
2.	Canadian Shield	$900f^{0.2}$	Hasegawa (1985)
3.	Eastern Canada	$1100f^{0.19}$	Chun et al. (1987)
4.	Eastern United States	$800f^{0.32}$	Gupta and McLaughin (1987)
5.	Central Appalachia	$570f^{0.46}$	Shi et al. (1996)
6.	Adirondack Mountains	$905f^{0.4}$	Shi et al. (1996)
7.	New England	$460f^{0.4}$	Pulli (1984)
8.	Baltic Shield	$125f^{1.08}$	Kvamme and Havskov (1989)
9.	Southern Italy	$62.5f^{0.7}$	Tuve et al. (2006)
10.	Central Iran	$53f^{1.02}$	Ma'hood et al. (2009)
11.	Guerrero, Mexico	$47f^{0.87}$	Rodriguez et al. (1983)
12.	Dead Sea	$65f^{1.05}$	Van Eck (1988)
13.	Parkfield	$79f^{0.74}$	Hellweg et al. (1995)
14.	Friuli, Italy	$80f^{1.1}$	Rovelli (1982)
15.	South Spain	$155f^{0.89}$	Ibanez et al. (1990)
16.	Norway	$120f^{1.09}$	Kvamme and Havskov (1989)
17.	Eastern Indian Shield	$313.2f^{0.73}$	Present study

Adirondack Mountains (Shi et al. 1996), and New England (Pulli 1984) is noted at lower frequencies and increases further gradually. The attenuation values though are found to be higher than Southern Italy (Tuve et al. 2006), Central Iran (Ma'hood et al. 2009), Guerrero, Mexico (Rodriguez et al. 1983), Dead Sea (Van Eck 1988), Parkfield (Hellweg et al. 1995), Friuly, Italy (Rovelli 1982), and South Spain (Ibáñez et al. 1990) for all the frequencies, becomes lesser than Baltic Shield (Kvamme and Havskov 1989), Norway (Kvamme and Havskov 1989) at higher frequency. This worldwide comparison also advocates similar view of moderate to higher attenuation of seismic shear wave for the Eastern Indian Shield region.

The coda-Q estimates in the present study is strongly dependent on frequency and follow a power law relationship of $Q_c = Q_0 f^n$. The moderate value of n obtained in this study clearly correlates with intermediate value of Q_c in the low frequency range (up to 3 Hz) and relatively higher Q_c value in the higher frequency range (cf. Fig. 3). The relatively moderate Q_c at the lower frequency range can be attributed to the loss of energy due to the presence of numerous heterogeneities with decreasing rock-strength. The widely varying coda Q possibly accounts for either higher heterogeneity distributed widely or concentrated subsurface deformation in the study area. Occasionally, low coda Q is associated with the zones of concentrated deformation. High heat flow of $\sim$75 mWm^{-2}, high strain rate (ε) of 2–3 × 10^{-9} per year, and high Poisson's ratio of $\sim$0.31 of the constituent rocks for the crust beneath this area (Sharma et al. 2015 and references therein) apparently comply with such deformation. This generally leads to ductile failure at low stress level, and the fractures are apparently weakened by fluid (water). Khan et al. (2009) found a positive correlation between moment magnitude and seismic moment for the Eastern Indian Shield region, and failed to find any relation of moment magnitude with stress drops or source radii which support the existence of higher degree of subsurface lateral heterogeneity. Several sub-basins, plateaux, hills, shear zones, intervening numerous hot springs, fluid induced fractures, lineaments and intrusions of basic rocks are very common features in this part of Eastern India, and accounts for higher complexity in the geological formation beneath the study area. The occasional incidences of moderate magnitude earthquakes, namely, the 1868 Manbhum (M 5.7), 1868 Hazaribagh (M 5.0), 1934 North Bihar (M 8.0), 1958 Bihar, 1963 Ranchi (M 5.0) and 1969 Bankura (M 5.7) also corroborate the moderate to little higher tectonic level of the area, and comply with the moderate to higher n values obtained under the present study.

5 Limitation of the study

Although the long coda window has been chosen to provide a stable measure of the coda decay by smoothing out irregularities in the function $\ln(A(f,\ t)t)$; limited number of properly located events available in the present study was one of the main hindrances in constructing proper attenuation relation. Meaningful comparisons between stations are basically possible when one choose consistent parameters (window length, window end time) and events with similar depths and distances. However, we were not in a position to do this exercise with the limited dataset. There is only one broadband station recording earthquake events effectively over last many years, which constraints the comparison of Q_c values between different stations, and was not able to provide more detailed understanding of seismic wave attenuation for different locations. Further, the widely varying epicentral distances (95–437 km, Table 1) for sporadically distributed events results the higher variation of depth of back scattered waves; clearly limits our understanding for deeper information. However, the frequency dependence of average Q_c obtained through the expression of the form $Q_c = Q_0 f^n$ provide preliminary valuable information for the region.

6 Conclusions

We investigated the coda wave attenuation characteristics in the Eastern Indian Shield regions at five central frequencies 0.55, 3.0, 7.5, 12.5 and 20.0 Hz for three coda windows of 30, 40 and 50 s. The computed coda Q is found to be strongly dependent on frequency, and obeys a power law of $Q_c = 313.2f^{0.73}$. This indicates that the crustal part in the Eastern Indian Shield region is more attenuative because of concentrated deformation and associated faulting of the Gondwana graben. The rate of increase of Q_c with frequency is found to be comparable with other regions in India and around the world. The lower coda Q values at lower frequencies (1–3 Hz) is possibly due to the energy loss at heterogeneities and relatively higher Q values for the higher frequency band (>12 Hz) might be indicating more homogeneous deeper crustal layer (Mandal and Rastogi 1998). The higher Q values at higher lapse time are reflecting the propagation of backscattered body waves through the more homogeneous deeper parts of the lithosphere (Parvez et al. 2008).

Acknowledgments Authors are thankful to the Director, Indian School of Mines, Dhanbad for providing the infrastructural facilities. This work was financially supported by the Ministry of Earth Sciences, Govt. of India, New Delhi. The authors are thankful to Peter Varga and other anonymous reviewers for their critical comments and suggestions, which has improved the manuscript.

References

Aki K (1969) Analysis of Seismic coda of local earthquakes as scattered waves. J Geophys Res 74:615–631

Aki K (1980) Attenuation of shear-waves in the lithosphere for frequencies from 0.05 to 25 Hz. Phys Earth Planet Int 21:50–60

Aki K (1981) Source and scattering effects on the spectra of small local earthquakes. Bull Seismol Soc Am 71:1687–1700

Aki K, Chouet B (1975) Origin of coda waves: source, attenuation and scattering effects. J Geophys Res 80:3322–3342

Bhattacharjee N, Ray J, Ganguly S, Saha A (2012) Mineralogical Study of Gabbro-Anorthosite from Dumka, Chotanagpur Gneissic Complex, Eastern Indian Shield. J Geol Soc India 80:481–492

Bilham R, Bendick R, Wallace K (2003) Flexure of the Indian plate and intraplate earthquakes. Proc. of the Indian Academy of Science. Earth Planet Sci 112:315–329

Bose MK (1999) Geochemistry of trhe metabasics and related rocks from the eastern part of the Proterozoic Singhbhum mobile belt, eastern India—Petrogenitic implications. Indian J Geol 71:213–234

Bose MK (2009) Precambrian Mafic Magmatism in the Singhbhum Craton, Eastern India. J Geol Soc India 73:13–35

Chatterjee N, Ghose NC (2011) Extensive Early Neoproterozoic high-grade metamorphism in north Chotanagpur Gneissic Complex of the Central Indian Tectonic Zone. Gond Res 20:362–379

Chun KY, West GF, Kokoski RJ, Samson C (1987) A novel technique for measuring Lg attenuation: results from eastern Canada between 1 and 10 Hz. Bull Seismol Soc Am 77:398–419

Dasgupta S, Mukhopadhyay M, Nandy DR (1987) Active transverse features in the central portion of the Himalaya. Tectonophys 136:255–264

Gao LS, Biswas NN, Lee LC, Aki K (1983) Effects of multiple scattering on coda waves in three dimensional medium. Pure appl Geophys 121:3–15

Ghose NC, Chatterjee N (2008) Petrology, Tectonic Setting and Source of Dykes and Related Magmatic Bodies in the Chotanagpur Gneissic Complex, Eastern India. In: Srivastava RK, Sivaji C, Chalapathi

Rao NV (eds) Indian Dykes: Geochemistry, Geophysics and Geochronology. Narosa Publ. House Pvt. Ltd, New Delhi, pp 471–493

Ghose NC, Mukherjee D (2000) Chotanagpur gneissgranulite complex, Eastern India—A kaleidoscope of global events. In: Trivedi AN, Sarkar BC, Ghose NC, Dhar YR (eds) Geology and Mineral Resources of Bihar and Jharkhand, Platinum Jubilee Commemoration Volume. Indian School of Mines, Institute of Geoexploration and Environment, Monograph 2, Dhanbad, Patna, pp 33–58

Gupta SC, Kumar A (2002) Seismic wave attenuation characteristics of three Indian regions. A comparative study. Curr Sci 82:407–413

Gupta IN, McLaughin KL (1987) Attenuation of ground motions in the Eastern United States. Bull Seismol Soc Am 77:366–383

Gupta SC, Singh VN, Kumar A (1995) Attenuation of coda waves in the Garhwal Himalaya, India. Phys Earth Planet Int 87:247–253

Hasegawa HS (1985) Attenuation of Lg waves in the Canadian shield. Bull Seismol Soc Am 75:1569–1582

Havskov J, Ottemoller L (2003) SEISAN: The earthquake analysis softwares for Windows, Solaris and Linux, Version 8.0. Institute of Solid Earth Physics. University of Bergen, Norway

Havskov J, Malone S, McClury D, Crosson R (1989) Coda-Q for the state of Washington. Bull Seismol Soc Am 79:1024–1038

Hellweg M, Spudich P, Fletcher JB, Baker LM (1995) Stability of coda Q in the region of Parkfield, California: view from the U.S. geological survey Parkfield dense seismograph array. J Geophys Res 100:2089–2102

Ibáñez JM, Pezzo ED, De Miguel F, Herriaz M, Alguacie G, Morales J (1990) Depth dependent seismic attenuation in the Granada zone (Southern Spain). Bull Seismol Soc Am 80:1232–1244

Jin A, Aki K (1988) Spatial and Temporal correlation between coda Q and seismicity in China. Bull Seismol Soc Am 78:741–769

Jin A, Aki K (1989) Spatial and temporal correlation between coda Q^{-1} and seismicity and its physical mechanism. J Geophys Res 94:14041–14059

Khan PK, Chakraborty S, Srivastava VK, Prasad R (2009) Seismicity, source parameters and scaling relationships for the eastern part of Eastern Indian Shield region. Indian Miner 61:65–74

Kumar N, Parvez IA, Virk HS (2005) Estimation of Coda wave attenuation for NW Himalayan region using local earthquakes. Phys Earth Planet Inter 151:243–258

Kumar CHP, Sarma CSP, Shekar M, Chadha RK (2007) Attenuation studies based on local earthquake coda waves in the southern Indian peninsular shield. Nat Hazards 40:527–536

Kvamme LB (1985) Attenuation of seismic energy form local events in Norwegian areas, M. Sc. Thesis, University of Bergen, Norway

Kvamme LB, Havskov J (1989) Q in Southem Norway. Bull Seismol Soc Am 79:1575–1588

Ma'hood M, Hamzehloo H, Doloei GJ (2009) Attenuation of high frequency P and S waves in the crust of the East-Central Iran. Geophys J Int 179:1669–1678

Mahadevan TM (2002) Geology of Bihar and Jharkhand. Geol Soc India, Bangalore

Mandal P, Rastogi BK (1998) A frequency-dependent relation of coda Q_c for Koyna-Warna region, India. Pure appl Geophys 153:163–177

Mandal HS, Khan PK, Sukla AK (2013) Shear Wave attenuation characteristics over the Central India Tectonic Zone and its surroundings. J Asian Earth Sci 73:440–451

Mitchell B (1981) Regional variation and frequency dependence of Q_β in the crust of the United States. Bull Seismol Soc Am 71:1531–1538

Mukhopadhyay S, Sharma J (2010) Crustal scale detachment in the Himalayas: a reappraisal. Geophys J Int 183:850–886

Naqvi SM, Rogers JJW (1987) Precambrian Geology of India. Oxford University Press Inc, New York, p 223

Parvez IA, Sutar AK, Mridula M, Mishra SK, Rai SS (2008) Coda Q Estimates in the Andaman Islands Using Local Earthquakes. Pure Appl Geophys 16:1861–1878

Paul A, Gupta SC, Pant CC (2003) Coda Q estimates for Kumaun Himalaya. Proc Indian Acad Sci (Earth Planet Sci) 112:569–576

Pujades L, Canas JA, Egozcue JJ, Puigvi MA, Pous J, Gallart J, Lana X, Casas A (1991) Coda Q distribution in the Iberian Peninsula. Geophys J Int 100:285–301

Pulli JJ (1984) Attenuation of coda waves in New England. Bull Seismol Soc Am 74:1149–1166

Rautian TG, Khalturin VI (1978) The use of the coda for the determination of the earthquake source spectrum. Bull Seismol Soc Am 68:923–948

Rodriguez M, Havskov J, Singh SK (1983) Q from coda waves near Petatlán, Guerrero, Mexico. Bull Seismol Soc Am 73:321–326

Roecker SW, Tucker B, King J, Hartzfield D (1982) Estimates of Q in Central Asia as a function of frequency and depth using the coda of locally recorded earthquakes. Bull Seismol Soc Am 72:129–149

Rovelli A (1982) On the frequency dependence of Q in Friuli from short period digital records. Bull Seismol Soc Am 73:2369–2372

Sarkar SN (1982) Precambrian tectonic evaluation of eastern India: a model of conversing microwplates. Tectonophysics 86:363–397

Sarkar SN, Saha AK (1977) Present status of the Precambrian stratigraphy, tectonics and geochronology of Singhbhum, Keonjhar, Mayurbhanj region, Eastern India. Indian J Earth Sci 4:37–55

Sarkar SN, Saha AK, Boelrijk NAIM, Hebada EH (1979) New data on the geochronology of the Older Metamorphic Group and the Singhbhum Granite of Singhbhum-Keonjhar-Mayurbhanj region, Eastern India. Indian J Earth Sci 6:32–51

Sato H (1977) Energy propagation including scattering effect. J Phys Earth 25:27–41

Sato H, Fehler M (1998) Wave Propagation and Scattering in the Heterogeneous Earth. AIP Press/Springer, New York, pp 1–308

Sharma B, Gupta AK, Devi DK, Kumar D, Teotia SS, Rastogi BK (2008) Attenuation of high frequency seismic waves in Kachchh region, Gujarat, India. Bull Seismol Soc Am 98:2325–2340

Sharma B, Kumar D, Teotia SS, Rastogi BK, Gupta AK, Prajapati S (2012) Attenuation of coda waves in the Saurashtra region, Gujarat (India). Pure appl Geophys 169:89–100

Sharma NK, Khan PK, Bhukta KK (2015) Nature of the Moho in the mid-eastern part of the Chotanagpur Plateau, India, from a receiver function perspective. J. Geosci doi/, Arab. doi:10.1007/s12517-014-1648-8

Shi J, Kim WY, Richards PG (1996) Variability of crustal attenuation in the northeastern United States from Lg waves. J Geophys Res 101:25231–25242

Shin TC, Herrmann RB (1987) Lg attenuation and source studies using 1982 Miramichi data. Bull Seismol Soc Am 77:384–397

Singh SK, Herrmann RB (1983) Regionalization of crustal coda Q in the continental United States. J Geophys Res 88:527–538

Singh SK, Ordaz M, Dattatrayam RS, Gupta HK (1999) A Spectral Analysis of the 21 May 1997 Jabalpur India earthquake ($M_w = 5.8$) and estimated of ground motion from future earthquakes in the Indian Shield region. Bull Seismol Soc Am 89:1620–1630

Singh SK, Garcia D, Pacheco JF, Valenzula R, Bansal BK, Dattatrayam RS (2004) Q of the Indian Shield. Bull Seismol Soc Am 94:1564–1570

Tuve T, Bianco F, Ibáñez J, Patanè D, Pezzo ED, Bottari A (2006) Attenuation study in the Straits of Messina area (southern Italy). Tectonophysics 421:173–185

Udías A (1999) Principles of seismology. Cambridge University Press, The Edinburgh Building, Cambridge, p 475

Valdiya KS (1976) Himalaya transverse faults and their parallelism with subsurface structures of north Indian planes. Tectonophys 32:353–386

Van Eck T (1988) Attenuation of coda waves in the Dead Sea region. Bull Seismol Soc Am 78:770–779

Weaver BL (1990) Early Precambrian basic rocks of India. In: Hall RP, Hughes DJ (eds) Early Precambrian basic magmatism. Blackie, Glasgow, pp 339–351

Wu RS, Aki K (1988) Multiple Scattering and Energy Transfer of Seismic Waves—Separation of Scattering Effect from Intrinsic Attenuation, II, Application of the Theory to Hindu-Kush Region. Pure Appl geophys 128:49–80